THE EFFECT OF ADDING A SECOND NOTCH IN THE STRESS REGION OF AN EXISTING NOTCH

by

LAWRENCE S. CHIEN

Diploma, Taiwan Provincial Institute of Agriculture, 1965
B. Sc., College of Engineering, K. S. U., Manhattan, Ks. 1970

A MASTER'S THESIS

submitted in partial fulfillment of the

requirements for the degree

MASTER OF SCIENCE

Department of Mechanical Engineering

KANSAS STATE UNIVERSITY
Manhattan, Kansas

1972

Approved by:

Major Professor

TABLE OF CONTENTS

	Page
INTRODUCTION	1
PREVIOUS WORK	4
EXPERIMENTAL WORK	7
Model Preparation	7
Calibration Procedure	7
Testing Procedure	9
Bending Tests	10
Tension Tests	10
Stress Concentration Factor	11
EXPERIMENTAL RESULTS	12
DISCUSSION OF RESULTS	21
CONCLUSION	23
RECOMMENDATIONS	24
BIBLIOGRAPHY	25
APPENDIX I	26
APPENDIX II	32
ACKNOWLEDGEMENTS	36

LIST OF FIGURES

Figure		Page
1.	Photoelastic Model	3
2.	Circular Polarescope with Test Specimen Loaded in Bending	8
3.	Fringe Patterns for Specimen Loaded in Bending	13
4.	Resulting Curves of K_{sup}/K vs r/R, Bending	17
5.	K^*_{sup} and K_{sup} vs r/R, $\theta = 45^o$, Bending	18
6.	Resulting Curves (K_{sup}/K vs r/R), Tension	20
7.	Bending Calibration Model	28
8.	Fringe Order vs Distance from Neutral Axis of the Calibration Model	29
9.	Tension Calibration Model	32
10.	Calibration Curve in Tension	32
11.	Variation of N with x/L, r = 5/64 inch, $\theta = 30^o$, Bending	34
12.	Variation of N with P in Tension	36

LIST OF TABLES

Table		Page
1.	Fringe Order vs Load - Bending	12
2.	Stress Concentration Factors - Bending	16
3.	Stress Concentration Factors, Tension	19
4.	Fringe Order Values in Bending Calibration	28
5.	Load-fringe Order, Calibration Model in Tension	31
6.	Fringe Order Values, Bending Test	33
7.	Fringe Order-load, Tension Test	36

NOMENCLATURE

h	=	thickness of model in inches
w	=	width of model in inches
R	=	radius of groove in inches
r	=	radius of notch in inches
θ	=	angle of orientation of notch
x	=	distance from center line to the fringe
l	=	distance from center line to the root of the groove
p	=	applied load (dial reading in pounds)
N	=	fringe order
M	=	bending moment in in.-lbs.
Z	=	modulus of section in cubic inches
$\sigma_{nom.}$	=	nominal stress in psi.
$\sigma_{max.}$	=	maximum stress in psi.
f_σ	=	material fringe value in psi./in./fringe
K	=	stress concentration factor for groove alone
K_{sup}	=	stress concentration factor with notches superposed
K^*_{sup}	=	maximum stress concentration factor inside the secondary notches

INTRODUCTION

The research reported here is concerned with the effect of superimposing stress raisers, semicircular notches, on grooves with existing stress concentration.

The significance of stress concentrations in the domain of strength of materials is formally established. Strength reduced in a single discontinuity, such as a fillet, a hole, or a notch----, etc., is well known. A further reduction of strength results if two stress raisers are superimposed one on the other. Some investigations of studying this effect of superposition of stress raisers concluded that the product of the two single stress concentration factors was a close approximation for the net effect in the case where the second notch was superimposed on the first one at the point of maximum stress. In other investigations the product was found to be lower than the resultant stress concentration factor as calculated above. The stress concentration factors are different in tension than in bending for the same model, hence both need to be determined.

Very little has been reported on work with a secondary notch not located at the point of maximum stress of the first notch. Mr. Sallam started the investigations in this area and this thesis presents the results of the continuation of his work. He showed that at the minimum section (0-0') of Fig. 1, the stress is affected by the second notches at certain orientation angles. The stress concentration factor at point 0 or 0' of the section increases as r/R (the ratio of the second notch radius to the groove radius) decreases for the same geometry. This investigation concentrated on finding the effect of second notches at various orientation angles and the stress concentration factor for smallest values of r/R possible.

Photo-elastic techniques were employed to obtain the necessary information. The resultant maximum stresses on the groove surface were computed and compared with the maximum stresses on the second notch surface. The relation of the resultant stress concentration factors and the geometrical parameters was then established.

THIS BOOK CONTAINS NUMEROUS PAGES WITH DIAGRAMS THAT ARE CROOKED COMPARED TO THE REST OF THE INFORMATION ON THE PAGE.

THIS IS AS RECEIVED FROM CUSTOMER.

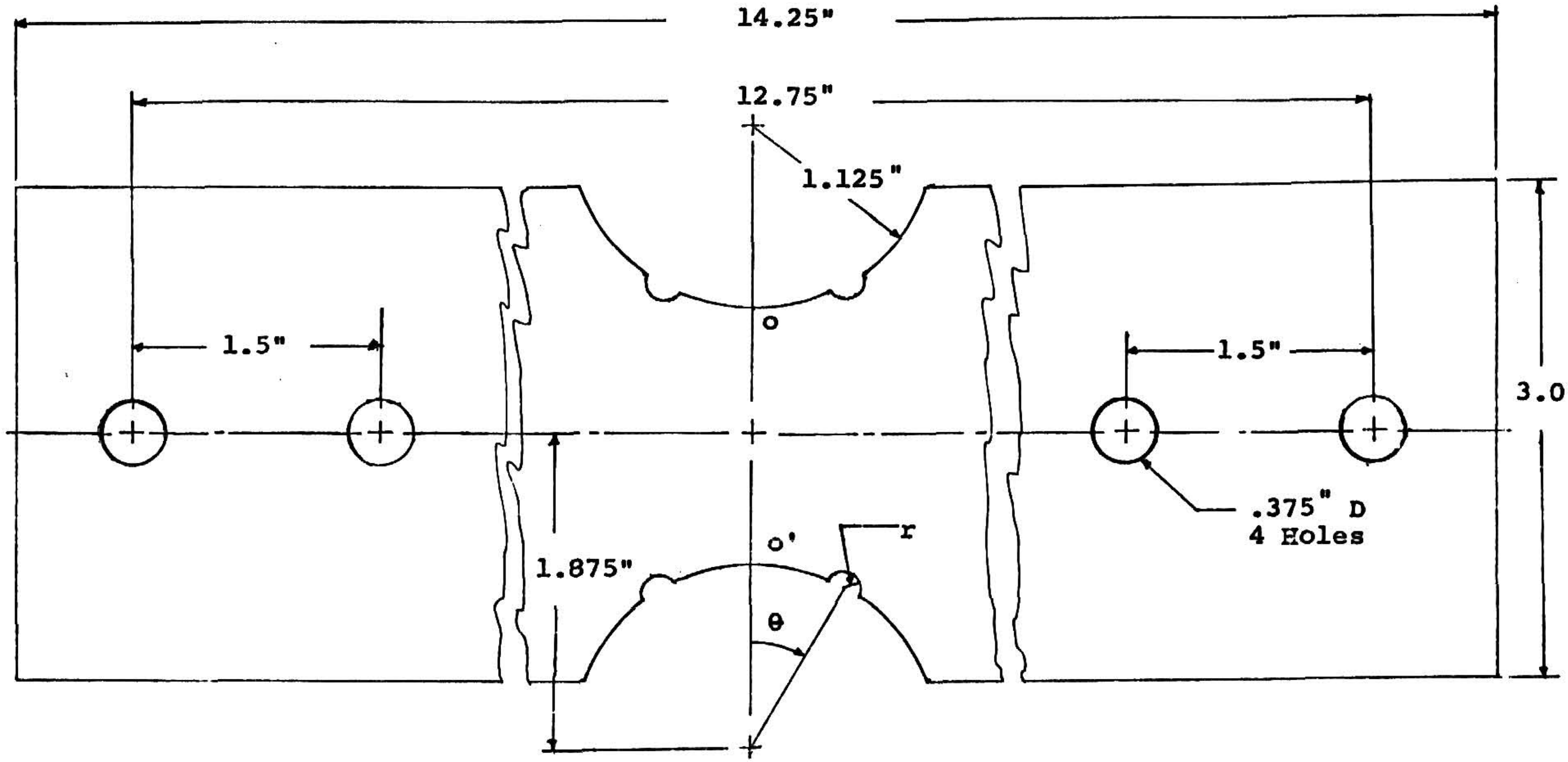

Fig. 1 Photoelastic Model

PREVIOUS WORK

S. Timoshenko and W. Dietz (1)*, in their study "Stress Concentration Produced by Holes and Fillets", concluded that in many practical cases a very high stress concentration is produced by holes, grooves, and sharp variation of cross-section. In design, effects of discontinuities are usually neglected for ductile materials subjected to static stresses, but not for brittle materials. For fluctuating loads, discontinuities weaken the part and must be considered in design with any material. Thus stress concentrations are of prime concern to the designer.

A. J. Durelli, R. L. Lake and E. Phillips (2), used photoelastic techniques in the study of "Stress Concentration Produced by Multiple Semicircular Notches Placed on Both Edges of A Plate under Uniaxial State of Stress". They concluded that the stress concentration factor decreases by adding more notches of the same geometry when the notches are close enough to influence each other but not superposed upon each other.

A. W. Mowbray (3), using electric resistance strain gages, found that the stress concentration factor of the combined effect of a semi-circular groove on a fillet range

---

* ( ) Refer to Bibliography

from 0.79 to 0.89 times the product of the theoretical factors for the groove and fillet alone. The probable reason why the combined effect was not close to the product of the individual effect is that the points of maximum stress of the fillet and groove were not coincident. Thus the real stress concentration factor at the root of the groove, due to the combined effect, would be nearer to the product of the value for the root of the groove and that for the corresponding subsurface value for the fillet.

F. W. Paul, Jr. and T. R. Faucett (4), in their photo-elastic study of the superposition of stress raising notches, proposed that if one stress raising notch is placed in the region of maximum influence of another notch the resulting stress concentration factor is close to the product of the stress concentration factors for the individual notches and they recommended the photo-elastic technique for this area of study because it has in the past provided an excellent check with theoretical results.

V. Vicentini (5) proposed a solution for two-dimension stress concentration factors for superposed semicircular notches symmetrically placed at the edges of a strip under pure tension. The equation proposed is based on some assumptions suggested by Mowbray and others. The solution for deep and shallow notches is based upon Neuber's equations. Vicentini performed a series of tests using strain gages and photo-elasticity and the results were then compared with the theoretical values of stress concentration factors. He concluded that the resulting stress concentration factor of superposed notches increases as the ratio of the notch radii decreases and is always lower than the product of the two single stress concentration factors.

M. M. Sallam (6), in his photelastic study of the superposition of stress raising notches, reported that the stress is affected by the superposed notches which are placed not at the points of maximum influence of the groove and the stress concentration factor at these points increases as the radius of the notches decreases.

EXPERIMENTAL WORK

Model Preparation

The research reported here was conducted in the Photoelastic Laboratory of the Department of Applied Mechanics at Kansas State University and covers a period of more than one semester.

The models used in all the tests were of Epoxy (PSM-5). This material was chosen because of its good machinability, freedom of residual stress, very low creep and time-edge effect, high modulus of elasticity and high sensitivity. The model, shown in Figure 1, was made with a very carefully machined templet using a high speed router. The secondary notches were cut and finished on a milling machine, using end mills ranging in size from 1/16 to 1/4 inches in diameter.

Calibration Procedure

Two calibration specimens were made from the material used - one for bending and the other for tension. They were tested for determining the material fringe value which is constant for any particular material and light source. The polariscope used in this research is shown in Figure 2. The reason for using this type of polariscope is that it employed

THIS BOOK CONTAINS NUMEROUS PICTURES THAT ARE ATTACHED TO DOCUMENTS CROOKED.

THIS IS AS RECEIVED FROM CUSTOMER.

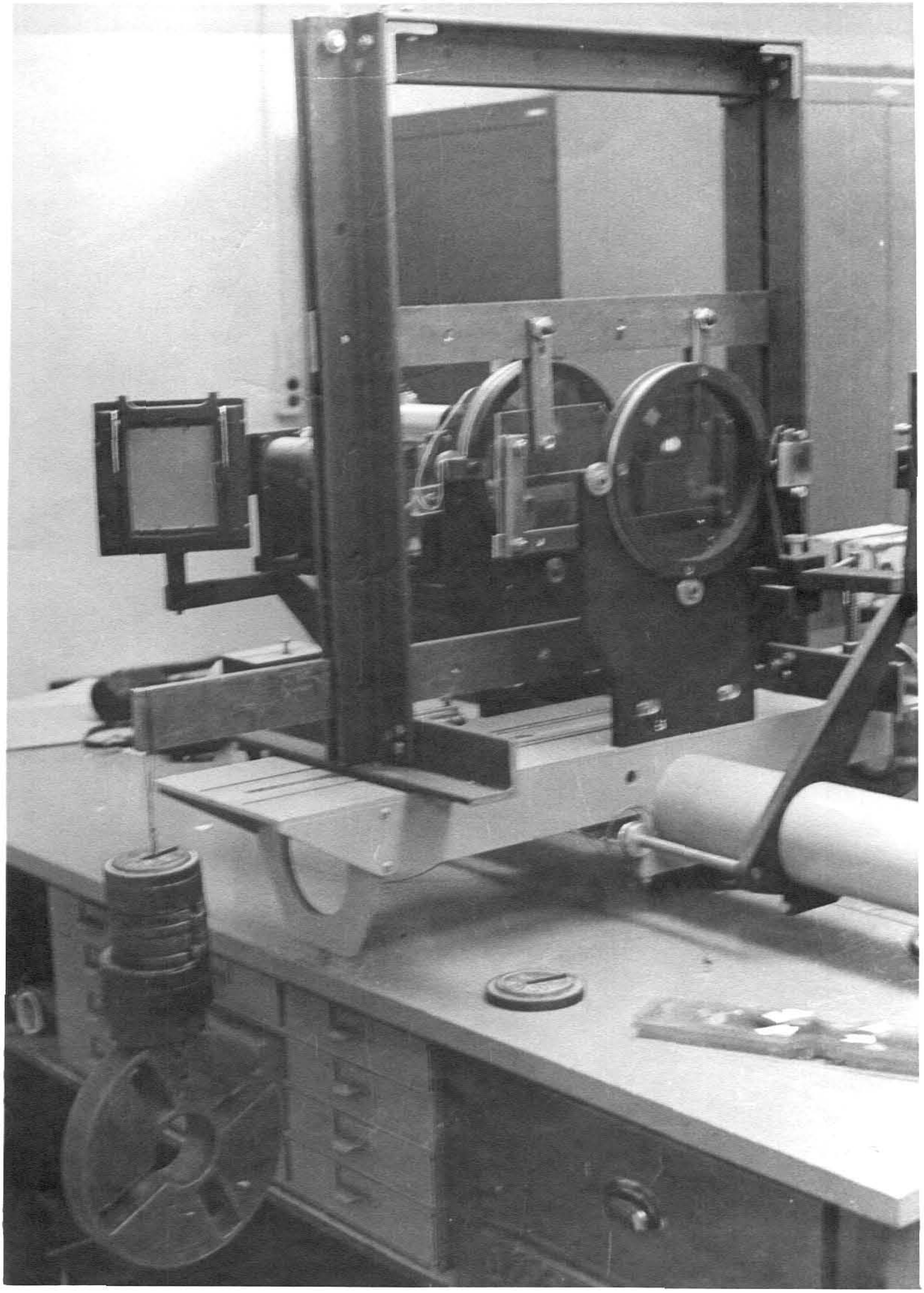

Fig. 2 Circular Polarescope with Test Specimen
Loaded in Bending

a collimated mercury green monochromatic light which makes sharper fringe patterns in the model, resulting in clearer pictures. The specimen was mounted in the loading frame and loaded in incremental steps. The details of both calibration tests are given in Appendix I. The results obtained for the material fringe value (f_σ) are 61.3 psi./in./fringe for bending and 64.8 psi./in./fringe for tension.

Testing Procedure

The models were, in turn, placed in the frame and loaded gradually while in the light field of the polariscope. The polariscope was adjusted to obtain a circularly polarized dark field (i.e., the polarizer was set perpendicular to the analyzer and quarter-wave plates were used). At a desirable loading, photographs were taken of the fringe patterns.

~~Sixteen~~ models were made besides the two calibration models. All the testing models had two large grooves symmetrically placed on opposite edges, and four same-size semi-circular notches symmetrically placed on the surface of the grooves. A detail drawing of one of the models, which had all notches symmetrical about its longitudinal centerline, is shown in Figure 1. The second notches (r) were of five sizes (1/32, 5/128, 7/128, 9/128, 3/32, 1/8 inches radii) and the orientation angles (θ) were in three positions (30, 45, 60 degrees from the point of minimum section of the groove). Thus, the size and orientation effects of the second notches on the stress concentration factors were observed.

Bending Tests

A fringe pattern was obtained by taking a photograph of the loaded model. Typical photographs are shown in Figure 3.

The fringe order at points 0 and 0' were then determined by extrapolation of the curve of the relation of fringe order and its relative position from the centerline of the model. Calculation for the maximum stresses at points 0 and 0', in one of the cases, is illustrated in Appendix II.

Tension Tests

The fringe patterns for models loaded in tension can not be used to determine the fringe order at boundaries as with the fringe patterns in bending. The fringes in tension patterns move from the boundaries (or from the edges) toward the center, then form a loop and depart from the central portion of the loaded area instead of accumulating on line 00'. Therefore, the model had to be loaded gradually in increments and the load for each succeeding fringe was recorded when it appeared on the boundary. The fringe orders were then plotted against the corresponding loads to obtain a curve. From the slope of the curve, the stress concentration factor was obtained. A calculation for one case is illustrated in Appendix II.

Stress Concentration Factor

The stress concentration factor in cases of pure tension is defined as the ratio of the maximum stress to the average stress in the same section through the discontinuity.

In the cases of bending, it is defined as the ratio of maximum stress to the stress computed by the elementary flexure formula (M/Z), where M and Z are the bending moment and the modulus of section, respectively.

EXPERIMENTAL RESULTS

The results of the bending tests were obtained from the fringe patterns as shown in Figure 3. The maximum boundary fringe orders at section 0-0', for various geometries, are in Table 1.

TABLE 1

Fringe Order vs Load - Bending

r/R	Load (lbs)	θ	Fringe Order
.028	148	30 45 60	6.30 5.90 5.30
.035	148	30 45 60	6.90 6.50 5.50
.049	203	30 45 60	9.00 8.30 7.40
.063	203	30 45 60	8.40 7.90 7.20
.083	234	30 45 60	9.70 8.60 8.00
.111	234	30 45 60	9.55 8.40 8.00

(a)

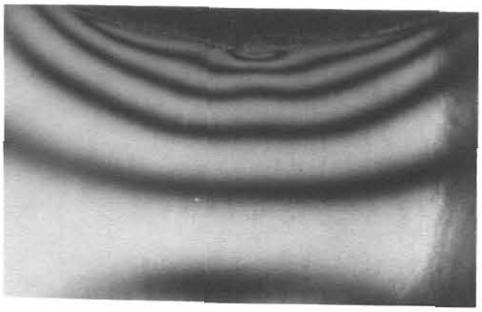

no notches, P=148 lbs.

(b)

$r= \frac{1"}{32}, \theta=30^{\circ}$, P=148 lbs.

(c)

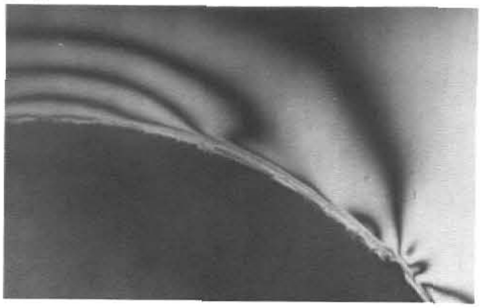

$r= \frac{1"}{32}, \theta=45^{\circ}$, P=148 lbs.

(d)

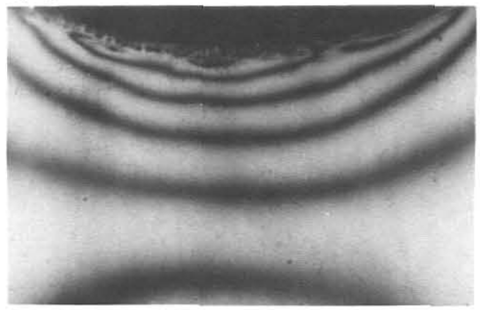

$r= \frac{1"}{32}, \theta=60^{\circ}$, P=148 lbs.

(e)

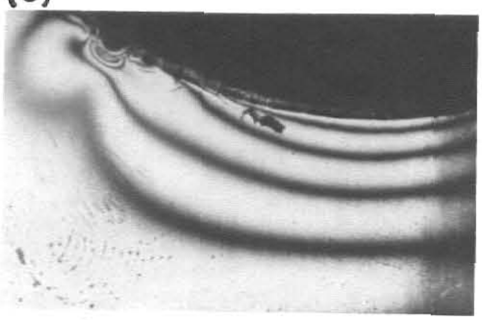

$r= \frac{5"}{128}, \theta=30^{\circ}$, P=148 lbs.

(f)

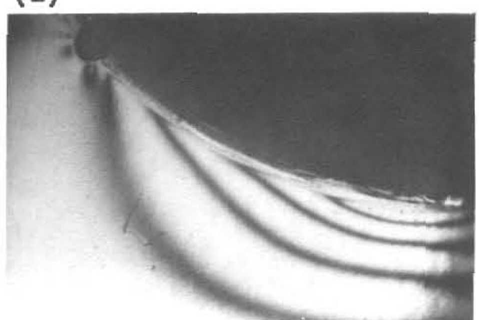

$r= \frac{5"}{128}, \theta=45^{\circ}$, P=148 lbs.

Fig. 3 Fringe Patterns for Specimen Loaded in Bending

(g)

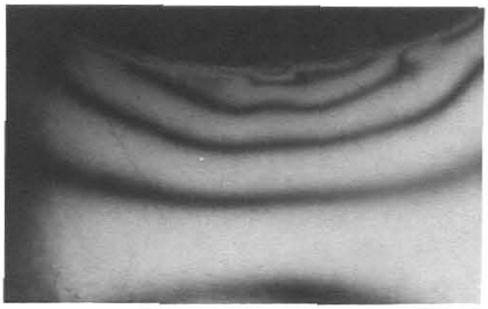

$r = \frac{5''}{128}$, $\theta=60^{\circ}$, P=148 lbs.

(h)

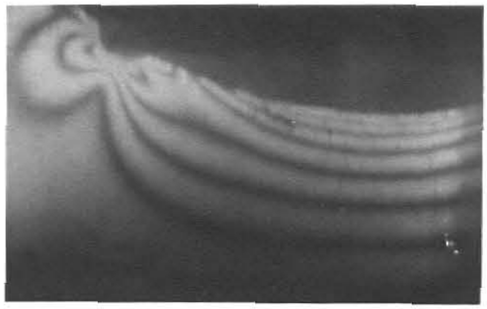

$r = \frac{7''}{128}$, $\theta=30^{\circ}$, P=203 lbs.

(i)

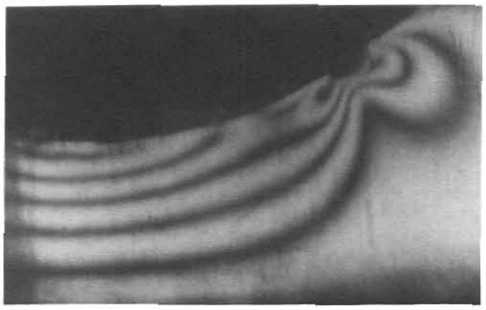

$r = \frac{7''}{128}$, $\theta=45^{\circ}$, P=203 lbs.

(j)

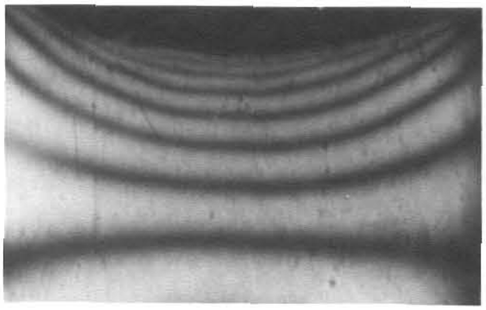

$r = \frac{7''}{128}$, $\theta=60^{\circ}$, P=203 lbs.

(k)

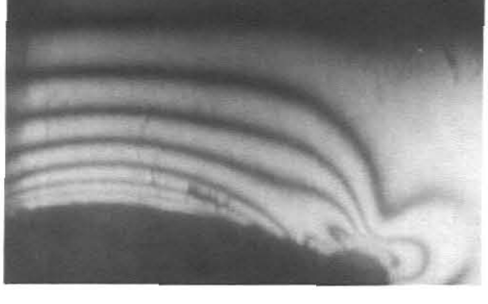

$r = \frac{9''}{128}$, $\theta=30^{\circ}$, P=203 lbs.

(l)

$r = \frac{9''}{128}$, $\theta=45^{\circ}$, P=203 lbs.

(m)

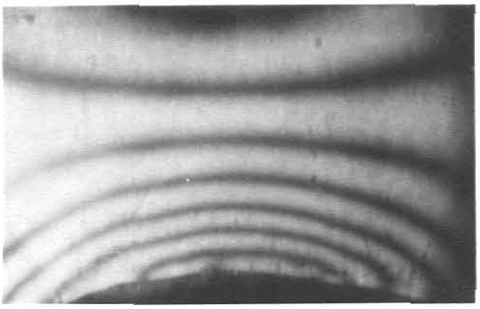

$r = \frac{9''}{128}, \theta = 60^{\circ}$, P=203 lbs.

(n)

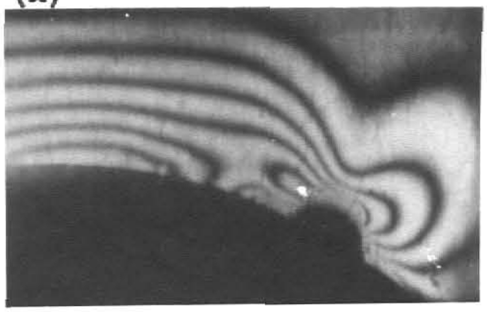

$r = \frac{3''}{32}, \theta = 30^{\circ}$, P=234 lbs.

(o)

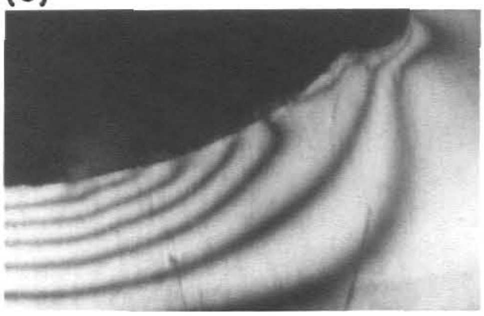

$r = \frac{3''}{32}, \theta = 45^{\circ}$, P=234 lbs.

(p)

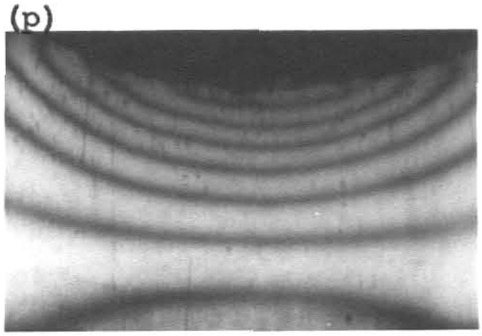

$r = \frac{3''}{32}, \theta = 60^{\circ}$, P=234 lbs.

(q)

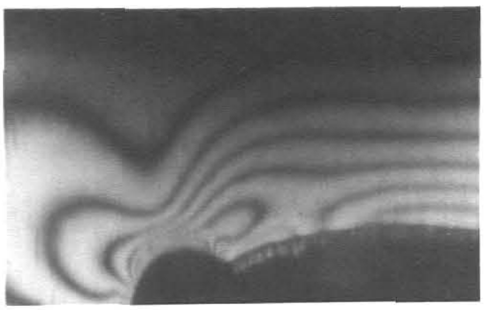

$r = \frac{1''}{8}, \theta = 30^{\circ}$, P=234 lbs.

(r)

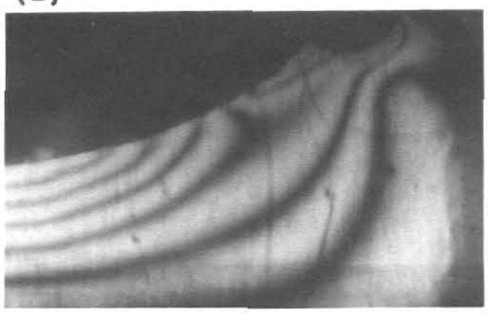

$r = \frac{1''}{8}, \theta = 45^{\circ}$, P=234 lbs.

The maximum stress concentration factors (K_{sup}) were calculated using Table 1. K_{sup} was then divided by K and plotted against r/R to give a series of resulting curves. They are tabulated in Table 2 and shown plotted in Figure 4.

TABLE 2

Stress Concentration Factors - Bending

r/R	θ	K_{sup}	K_{sup}/K
.000	30 45 60	1.09 1.09 1.09	1.00 1.00 1.00
.028	30 45 60	1.30 1.22 1.10	1.20 1.13 1.01
.035	30 45 60	1.43 1.34 1.14	1.32 1.23 1.05
.049	30 45 60	1.36 1.25 1.11	1.25 1.15 1.05
.063	30 45 60	1.29 1.26 1.09	1.19 1.11 1.00
.083	30 45 60	1.27 1.13 1.05	1.17 1.04 0.97
.111	30 45 60	1.25 1.12 1.05	1.15 1.03 0.97

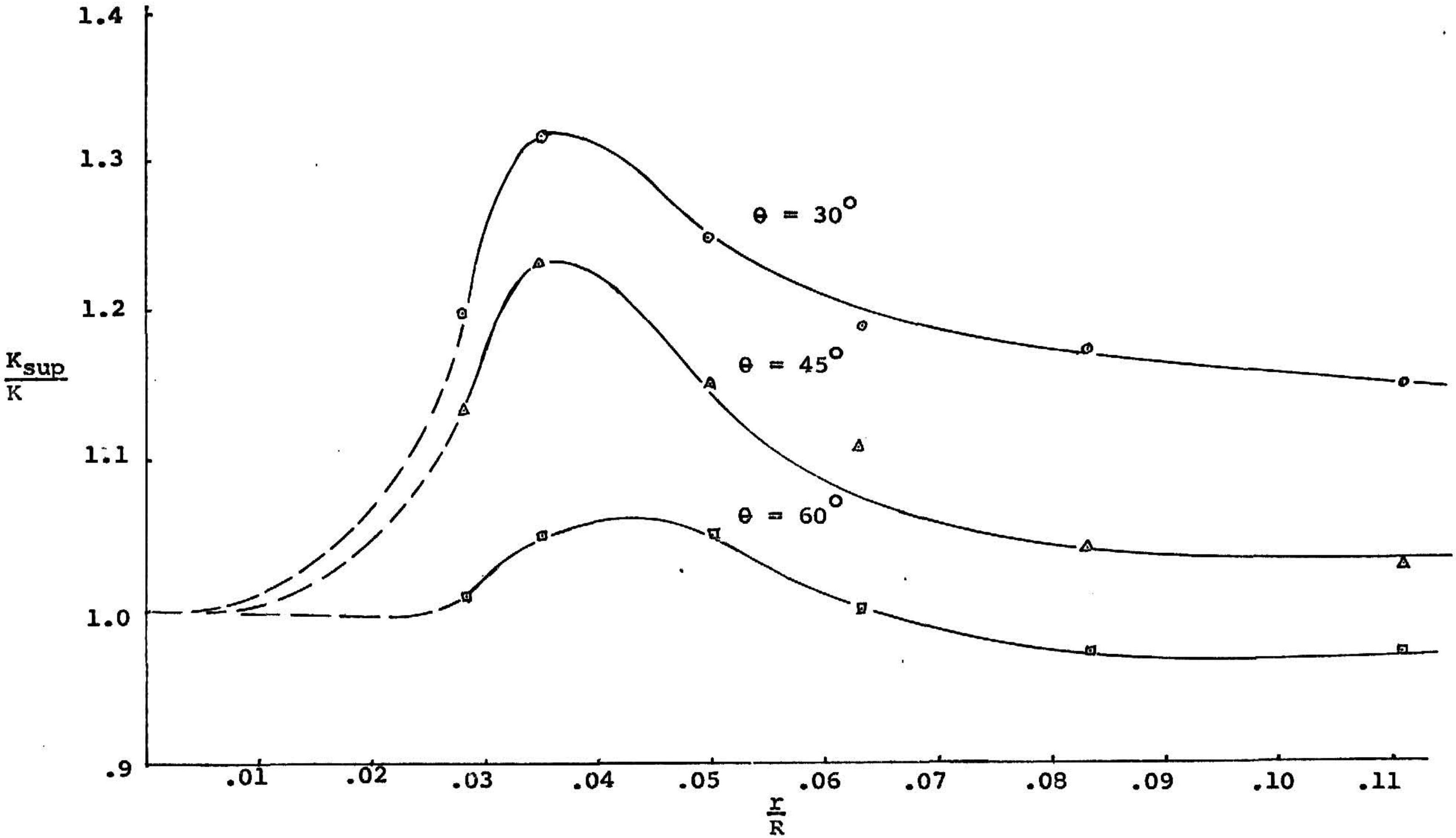

Fig. 4 Resulting Curves of K_{sup}/K vs r/R, Bending

Figure 5 shows the K_{sup} at section 0-0' and the K^*_{sup} at the boundary of second notch. As the fringe orders at the boundary of second notches are not clear and are difficult to extrapolate, the stress concentration factors at the boundary of secondary notches were calculated for the $\theta = 45^o$ and the second notch size from 3/16 inch to 7/16 inch only.

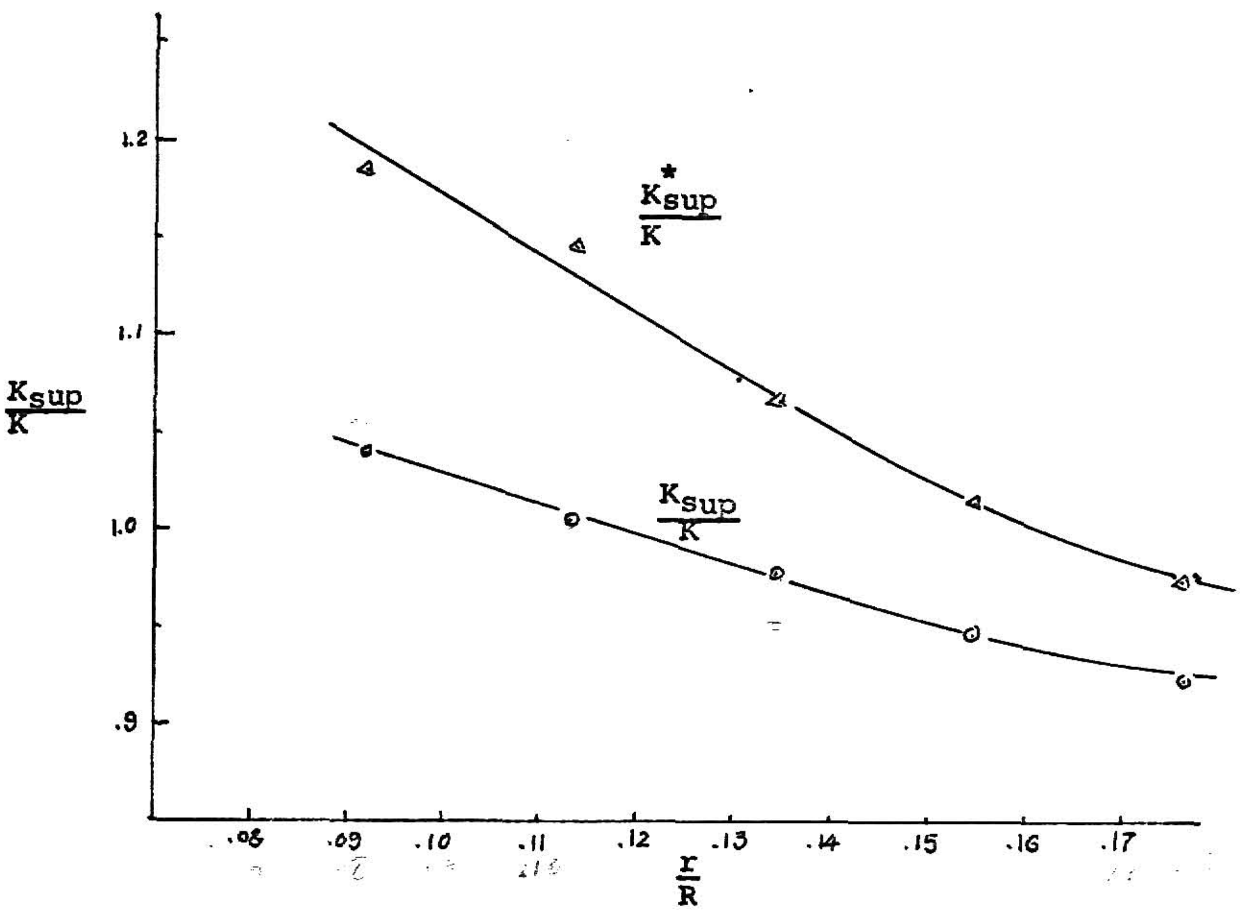

Fig. 5 K^*_{sup} and K_{sup} vs r/R, $\theta = 45^o$, Bending

For tension testing, the fringe orders at the boundaries and the corresponding loads were recorded. Table 3 shows the K_{sup} of variant geometries in tension.

Fig. 6 shows the resulting curves of K_{sup}/K vs r/R for three different orientation angles.

TABLE 3

Stress Concentration Factors, Tension

r/R	θ	P/N	K_{sup}	K_{sup}/K
.000	30	67.00	1.45	1.00
	45	67.00	1.45	1.00
	60	67.00	1.45	1.00
.028	30	67.00	1.45	1.00
	45	66.80	1.45	1.00
	60	66.80	1.45	1.00
.035	30	68.00	1.43	0.99
	45	67.30	1.44	0.99
	60	67.65	1.44	0.99
.049	30	66.80	1.45	1.00
	45	66.65	1.46	1.01
	60	67.30	1.44	0.99
.063	30	64.00	1.52	1.05
	45	66.35	1.47	1.01
	60	66.35	1.47	1.01
.083	30	61.40	1.58	1.09
	45	65.40	1.49	1.03
	60	65.70	1.48	1.02
.111	30	69.60	1.40	0.97
	45	68.30	1.42	0.98
	60	68.00	1.43	0.99

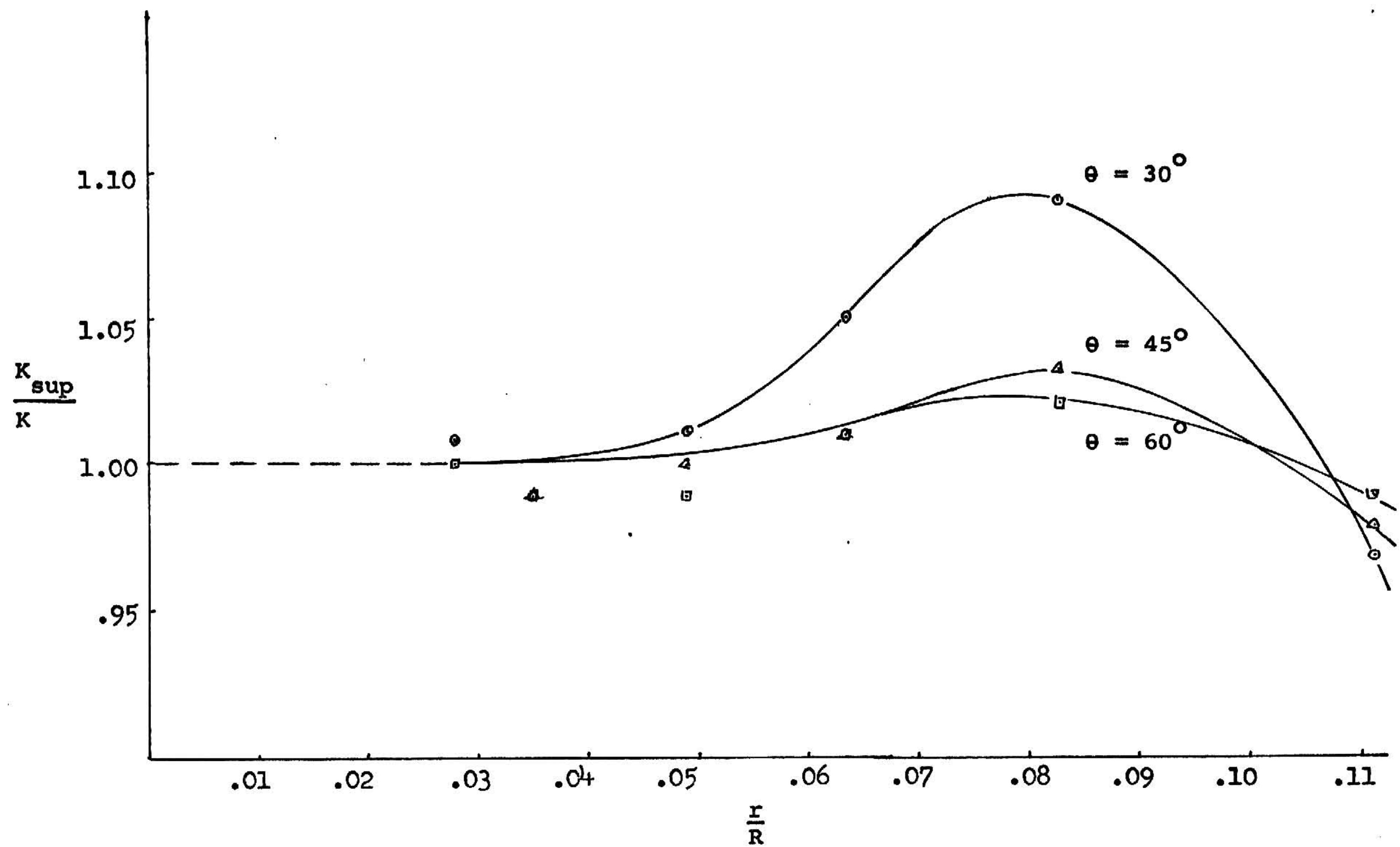

Fig. 6 Resulting Curves (K_{sup}/K vs r/R), Tension

DISCUSSION OF RESULTS

The resulting curves for bending test show that the smaller the orientation angle the higher the stress concentration factor will be. At about 60° of orientation angle the effect of secondary notch becomes small. It also shows that the stress concentration factors increase rapidly as the secondary notch radius increases in size from near zero to 5/128 inches and then decrease slowly as the size of secondary notch increases.

The peaks of the curves are located about r/R = .035, where the stress concentration factors are 1.43 for 30° of orientation angle, 1.34 for 45° of orientation angle, and 1.14 for 60° of orientation angle.

Figure 5 shows that the stress concentration factors inside the secondary notches (K^{*}_{sup}) are higher than those at the section of 0-0'. Although the stress concentration factor increases as the r/R decreases, the amount of the stress concentration factor inside the secondary notches over that at the section of 0-0' increases as the r/R decreases. Unfortunately, the fringe orders for r/R smaller than .083 are difficult to determine, the resulting curve of K^{*}_{sup} is plotted from r/R = .167 to r/R = .083 only. However, the increase of K^{*}_{sup} may continue to some critical size of secondary notch and then drops rapidly like the resulting curves of K_{sup}.

In the tension test, the K_{sup} increases very slowly as the size of the secondary notch increases up to 3/8 inches, then the K_{sup} decreases as the size of secondary notch increases. Within the range of $r/R = 0.05$, the resulting curves of the K_{sup} of various orientation angles change very little along the line of K. The deviation of these curves are considerably smaller than those in the bending test. Thus, the effect of secondary notch to the stress concentration is comparably small and can be neglected for r/R smaller than .05 and orientation angles bigger than 45^{o}. The fringe order inside the secondary notches was hard to record, therefore, the comparision of K_{sup} and K^{*}_{sup} was neglected. However, when the load increased to a certain amount, the increase of fringe order inside the secondary notches became rapid. Such a load for one case can be considered as a yield point in stress-strain diagram.

It is evidence that K_{sup} at 0-0' decreases when r gets large for both bending and tension. As the r increases the cross-section of secondary notch will decrease. The decrease of the cross-section of secondary notch affects the stress at 0-0'. When the cross-section of secondary notch decreases, the stress inside the secondary notch will increase while the stress at 0-0' decreases, when the cross-section of secondary notch decreases to close or smaller than the cross-section of 0-0', the K_{sup} at 0-0' will be smaller than K at 0-0' as the cross-section of secondary notch received more stress.

CONCLUSION

The results of this experiment are mostly in agreement with Sallam's experiment (6) of similar cases.

The values of stress concentration factors for the groove without notches are 1.08 for bending and 1.45 for tension which compared favorably with Froch's studies.

The effect of orientation angles is considerable. At 30^{o} of orientation angle, a maximum of stress concentration factor which is 1.43 occurs for r/R = .035 in bending. The deviation of bending resulting curves are higher than that of tension resulting curves, but both bending and tension curves decrease when r gets large. Secondary notch does not affect section 0-0' when r/R is smaller than .05 in tension.

The stress concentration factors inside the notches are higher than those at section 0-0' in bending for $\theta \leq 45^{o}$.

RECOMMENDATIONS

(1) The study in this area can be further extended to the effect of groove size and position (with the distance of center point of the groove from the centerline of the specimen and the radius of the groove as variables) so that it will be of value to engineers and designers for finding the stress concentration factor in any geometry of such a case.

(2) Other techniques such as the electric resistance strain gage method can be applied in this study to give a clear comparison of the resultant with that obtained from this experiment, hence the confidence of accuracy of the resulting data can be established.

(3) This problem may be treated by means of bipolar coordinates as a theoretical solution. A general discussion of stress and strain in bipolar coordinates was proposed by Jeffery (9). Ling (10) employed this technique in his study of "On the Stresses in A Plate Containing Two Circular Holes" and obtained a satisfactory solution.

BIBLIOGRAPHY

1. Timoshenko and Dietz, "Stress Concentration Produced by Holes and Fillets," Transactions, Am. Soc. Mech. Engrs., page 199, (1925)

2. A. J. Durelli, R. L. Lake and E. Phillips, "Stress Concentration Produced by Multiple Semi-Circular Notches in Infinite Plates Under Uniaxial State of Stress," Proc. Soc. Exp. Stress Anal., 1952, Vo. x, No. 2, pp. 53-64

3. A. Q. Mowbray, Jr., "The Effect of Superposition of Stress Raisers on Members Subjected to Static or Repeated Loads," Proceedings, Society for Experimental Stress Analysis, Vol. x, 1953, pp. 153

4. Paul, Jr., F. W. and T. R. Faucett, "The Superposition of Stress Concentration Factors," Trans. ASME, Jour. of Eng. for Ind. 1961, pp. 129-134

5. Vicentini, Vittorio, "Stress Concentration Factors for Superposed Notches," Experimental Mechanics, 1967, pp. 117-123

6. M. Sallam, a master's report of "Effect of Placing Second Stress Raising Notches in the Field of Influence of Existing Groove," M. E. K.S.U. 1969

7. Faires, V. M., "Design of Machine Elements," 4th Edition, 1965, Chapter 4

8. Frocht, M. M., "Photo-elastic Studies in Stress Concentration," Mechanical Engineering, 1936, Vo. 58, pp. 485-489

9. G. B. Jeffery, "Plane Stress and Plane Strain in Bipolar Coodinates," Phil. Trans. A 221, 265 (1921)

10. C. B. Ling,"On the Stresses in A Plate Containing Two Circular Holes," J. App. Phys. 19, 77 (1948)

APPENDIX I

Calibration of Material Fringe Value

Two calibration tests for the PSM-5 photo-elastic material fringe value (f_σ) were done.

Bending Calibration Test

The model as shown in Fig. 7 is the specimen for bending calibration test. The fringe pattern of the specimen at a certain load was a series of straight lines parallel to the neutral axis. Therefore, a resulting curve of the fringe order against the distance from the neutral axis was plotted which shows a straight line. The curve was then extrapolated to get the fringe at the boundary and with the load, f_σ was determined.

The following table shows the variation of fringe order (N) with the dimensionless distance (x/1) from the neutral axis on both sides.

TABLE 4

Fringe Order Values in Bending Calibration

N	x/l Tension Side	x/l Compression Side
1	.1570	.1746
2	.3380	.3740
3	.5180	.5375
4	.7020	.7230
5	.8740	.8980

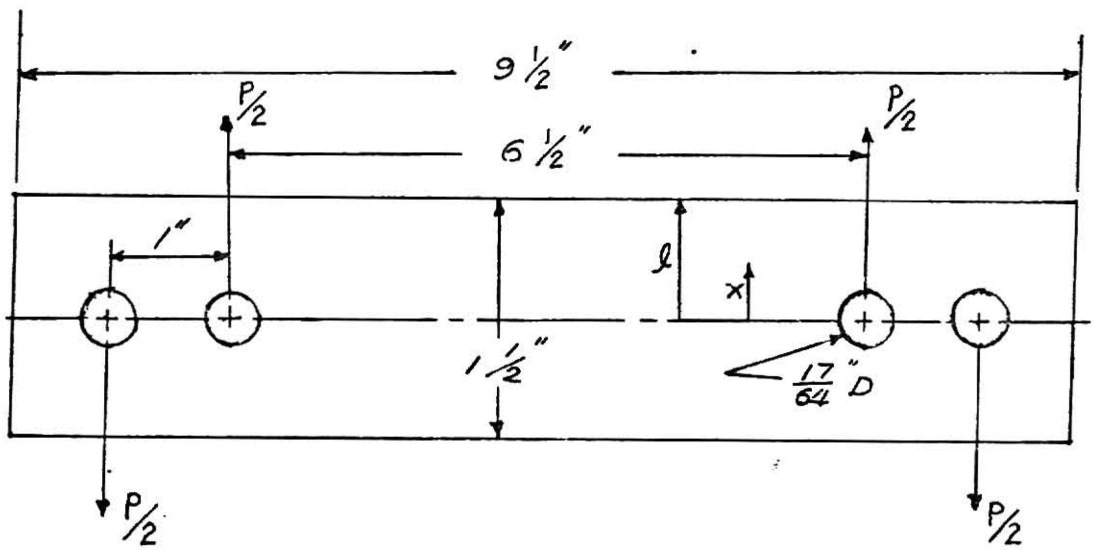

Fig. 7 Bending Calibration Model

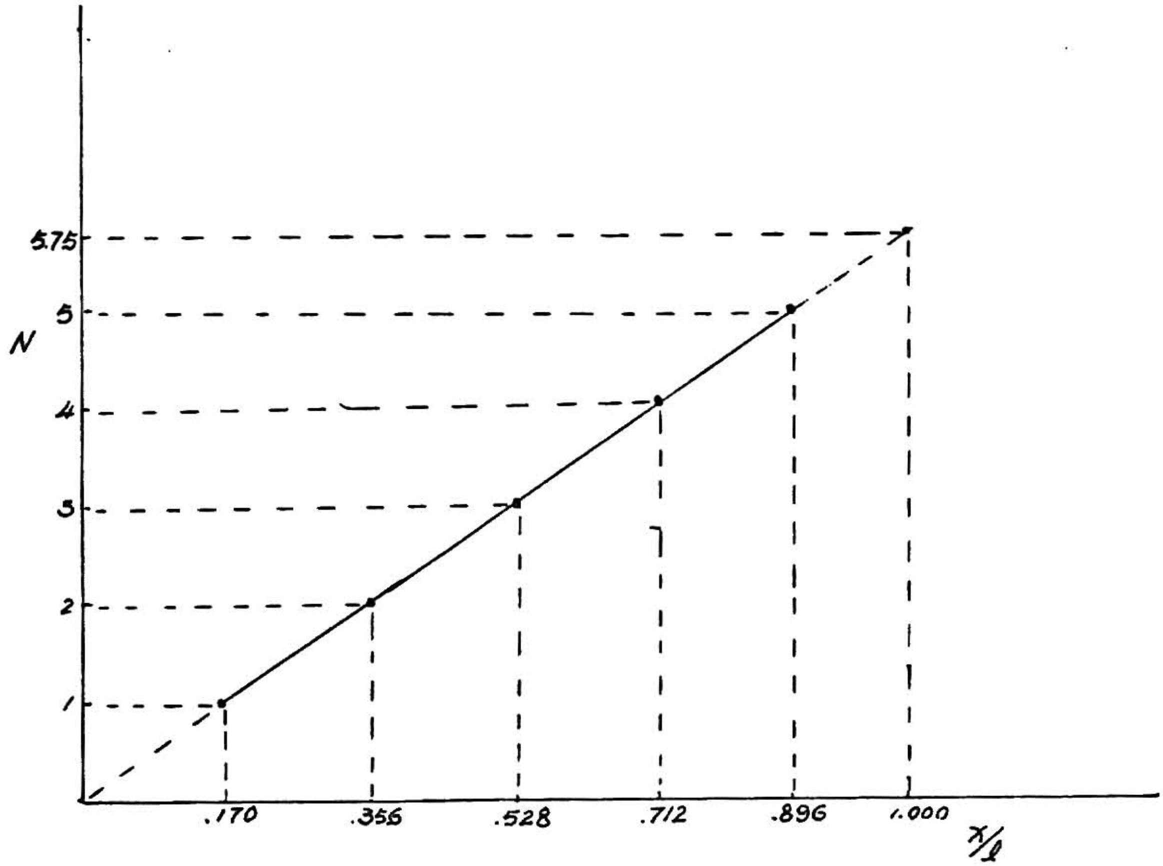

Fig. 8 Fringe Order vs Distance from Neutral Axis of the Calibration Model

The fringe order at the boundary of the calibration model was extrapolated as shown in Figure 8.

$$N = 5.75 \text{ fringes}$$

and

$$\text{Applied load} = 21 \text{ divisions}$$

$$= 21 \text{ div.} \times 12.62 \text{ lbs/div.}$$

$$= 265.02 \text{ lbs.}$$

$$M = \frac{265.02 \text{ lbs.}}{2} \times 1 \text{ in.}$$

$$= 132.51 \text{ in. lb.}$$

$$Z = \frac{hw^2}{6}$$

$$= \frac{(0.25 \text{ in.})\ (1.502 \text{ in.})^2}{6}$$

$$= 0.094 \text{ in}^3$$

$$\sigma_{nom} = \frac{M}{Z}$$

$$= \frac{132.51 \text{ lbs. in.}}{0.094 \text{ in}^3}$$

$$= 1409 \text{ psi.}$$

From photo-elasticity theory

$$\sigma_{max} - \sigma_{min} = \frac{Nf_\sigma}{h}$$

$\sigma_{min} = 0$ at boundaries, and $\sigma_{max} = \sigma$

$$1409 \text{ psi} = \frac{5.75 \text{ fringes} \cdot f_\sigma}{.25 \text{ in.}}$$

From which,

$f_\sigma = 61.3$ psi./in./fringe

Tension Calibration Test

The model shape is shown in Figure 9. When the model is introduced in the dark field of the scope, using pure light, the presence of the model without loading is of white. Then, as the load increases, the color of the model through the scope changes. The first fringe order is identified when the first red brown color appears in the scope and the second fringe order is the second carmine red, then the rest are pink red.

The load and the fringe order were recorded at the instant that the fringe appeared in the model. The following table is a record of the N and the corresponding P/W. Figure 10 shows the curve of this relation is a straight line and the slope of this curve is f_σ which is 64.8 psi./in./fringe.

TABLE 5

Load-Fringe Order, Calibration Model in Tension

N	Dial Reading	$\frac{P}{W} = \frac{\text{Dial Reading} \times 12.62}{0.759}$
1	3.45	57.4
2	7.18	119.4
3	11.10	184.6
4	15.17	252.2
5	19.05	316.7

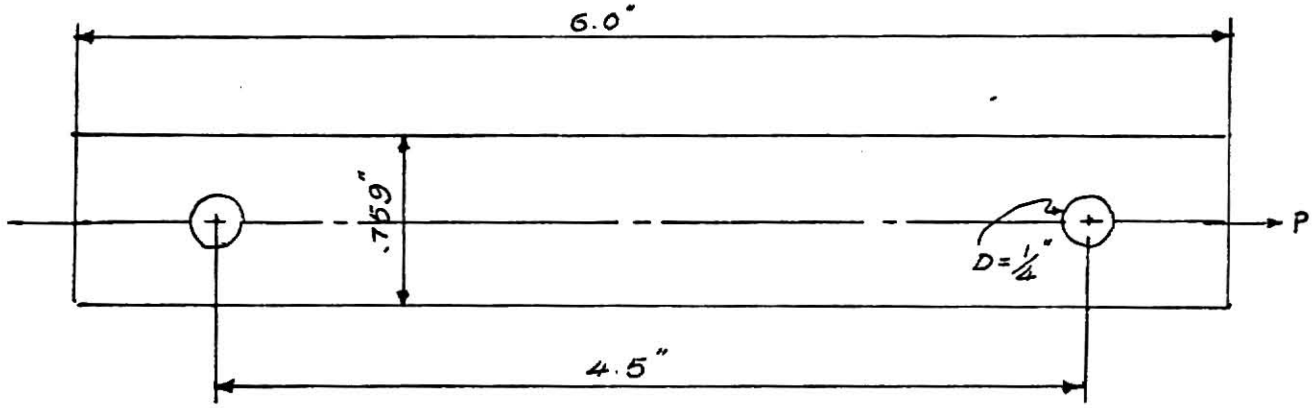

Fig. 9 Tension Calibration Model

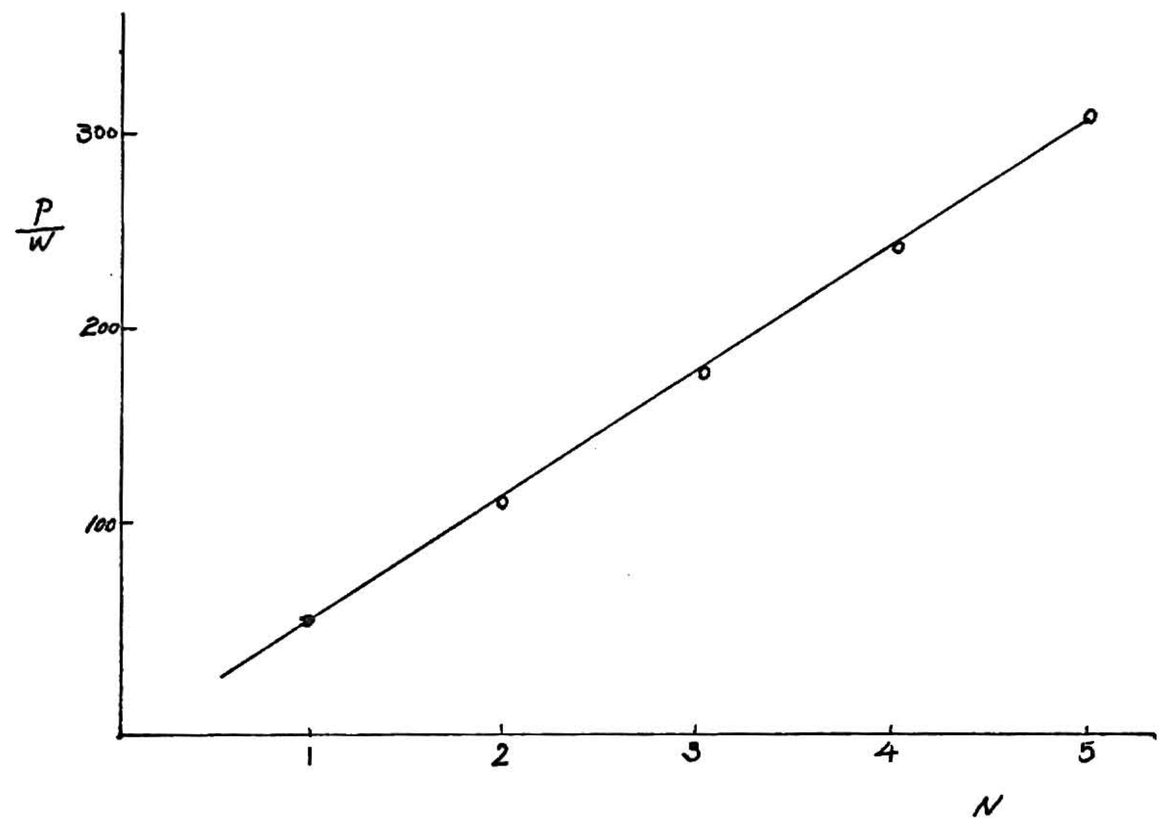

Fig. 10 Calibration Curve in Tension

APPENDIX II

Sample Calculations

Examples of how to determine the value of maximum stress concentration factor in bending and tension are presented here.

Bending

The following table shows fringe order and the corresponding distance from the reference point. The model was too big to obtain a photograph covering both the boundary and the centerline. Therefore, photographies which covered only the boundary were taken and the smallest fringe to be presented in the pattern picture was noted. In Fig. 11, the maximum fringe order was obtained by extrapolating the resulting curve to the boundary.

TABLE 6

Fringe Order Values, Bending Test

N	x/l	
	Tension Side	Compression Side
4.0	.456	.426
4.5	.620	.575
5.0	.724	.708
5.5	.816	.805
6.0	.880	.898
6.5	.946	.963

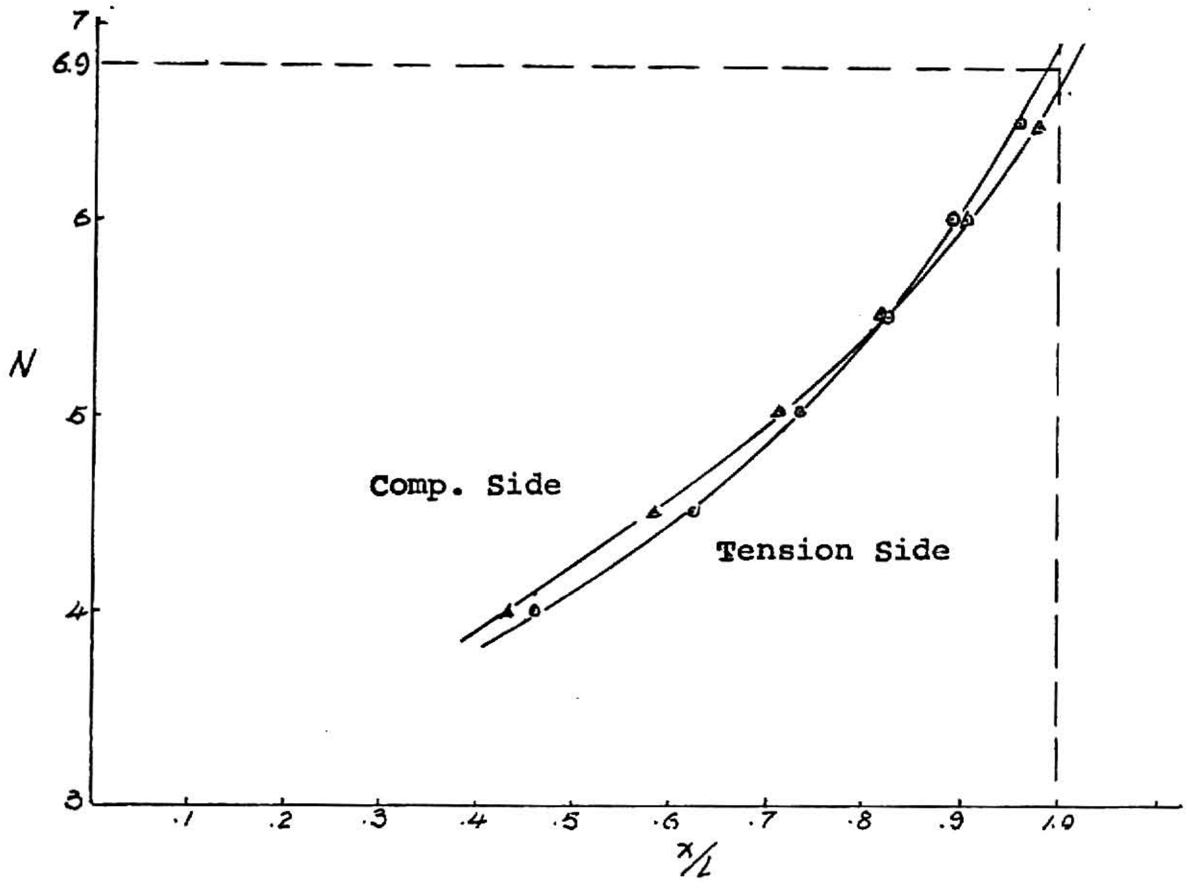

Fig. 11 Variation of N with x/L, r = 5/64 inch, $\theta = 30^{\circ}$, Bending

From Fig. 11 the average value of N at the boundary equals 6.9 fringes.

P = 148 lbs.

$$M = \frac{148 \text{ lbs.}}{2} \times 1.5 \text{ in.}$$

$$= 111 \text{ in. ib.}$$

$$Z = \frac{(0.25 \text{ in.}) \times 1.5 \text{ in}^2}{6} = 0.0936 \text{ in}^3$$

$$\sigma_{nom.} = \frac{M}{Z}$$

$$= 1187 \text{ psi}$$

$$\sigma_{max} = \frac{Nf\sigma}{h}$$

$$= \frac{6.9 \text{ fringe} \times 61.3 \text{ psi./in./fringe}}{0.25 \text{ in.}}$$

$$= 1692 \text{ psi}$$

$$K_{sup} = \frac{\sigma_{max.}}{\sigma_{nom.}} = \frac{1692}{1187}$$

$$= 1.428$$

Tension

As mentioned before, the fringes of tension do not accumulate on the 0-0' and from the theory a relation of the load and stress concentration factor was established.

That is

$$\sigma_{nom.} = \frac{P}{wh}$$

$$\sigma_{mas.} = \frac{Nf\sigma}{h}$$

$$K_{sup.} = \frac{max.}{nom.}$$

$$= \frac{Nf\sigma}{P/W}$$

Where $f\sigma/w$ is constant.

Therefore, a relation of N and p at the boundary will give the value of K_{sup}.

The following table shows the loads and the corresponding fringes that appeared at the boundary.

TABLE 7

Fringe Order-Load, Tension Test

N	Load			P = Load x 3.29
	One Side	Other Side	Average	
1.0	23.50	23.30	23.40	77.00
1.5	33.60	33.49	33.54	110.00
2.0	43.60	43.58	43.49	143.00
2.5	53.71	53.66	53.68	177.00
3.0	64.80	64.78	64.79	213.00

Figure 12 shows the curve of N vs P. with the slope of this curve, the K_{sup} was calculated. Slope = N/P = 1/68

K_{sup} = (fr x w) x N/P = (64.8 x 1.5)/68 = 1.43

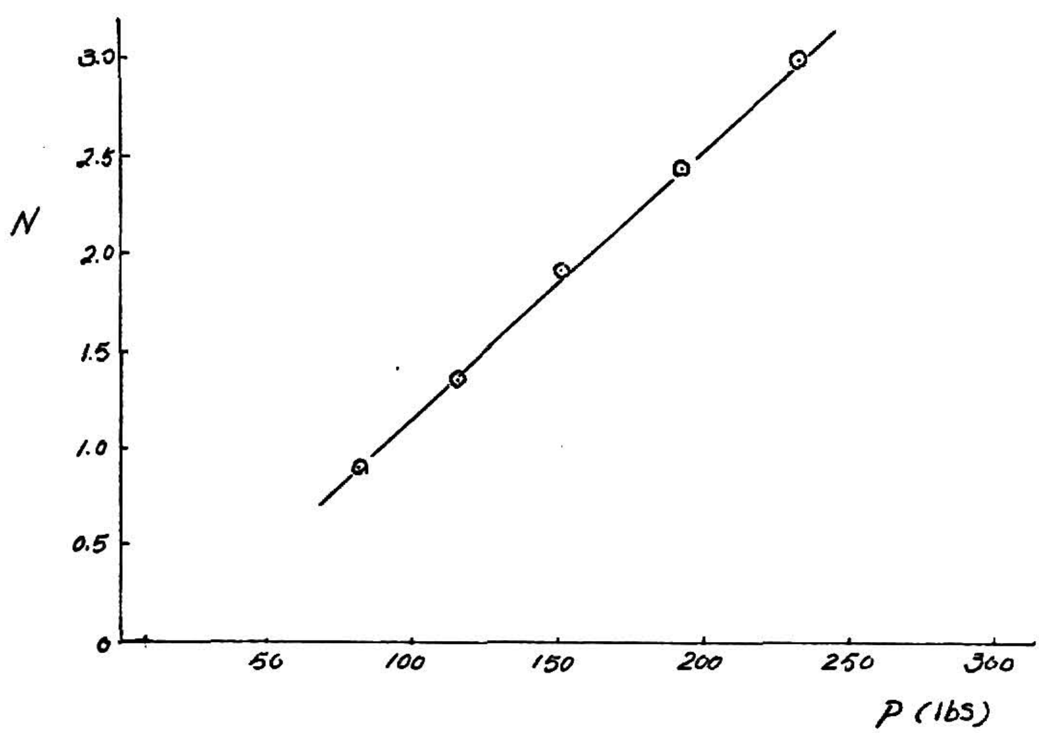

Fig. 12 Variation of N with P in Tension

ACKNOWLEDGEMENTS

The author acknowledges his appreciation to his advisor, Dr. J. C. Lindhlom, under whose direction the research was developed, and to Professor F. J. McCormick for his valuable suggestions.

THE EFFECT OF ADDING A SECOND NOTCH IN THE STRESS REGION OF AN EXISTING NOTCH

by

LAWRENCE S. CHIEN

Diploma, Taiwan Provincial Institute of Agriculture, 1965
B. Sc., College of Engineering, K. S. U., Manhattan, Ks. 1970

AN ABSTRACT OF A MASTER'S THESIS

submitted in partial fulfillment of the

requirements for the degree

MASTER OF SCIENCE

Department of Mechanical Engineering

KANSAS STATE UNIVERSITY
Manhattan, Kansas

1972

ABSTRACT

The purpose of this thesis is to find the effect of adding secondary notches in the stress region of the existing notch but not in the maximum stress point of the existing notch as that in the previous investigations.

Photo-elastic technique is applied and the models were of Epoxy (PSM-5). Sixteen testing models, besides two calibration models for determining the material fringe values of bending and tension, were made for observing the effect.

The results are in favour of the previous works and the peak values of stress concentration factor were found which are presented in the resulting curves.

Some further studies are recommended.